Proteomic comparison of the EWS-FLI1 expressing cells EF with NIH-3T3 and actin remodeling effect of (R/W)9 cell-penetrating peptide

Séverine Clavier, Françoise Illien, Sandrine Sagan, Gérard Bolbach, Emmanuelle Sachon

EuPA Open Proteomics 10 (2016) 1–8

Contents lists available at ScienceDirect

EuPA Open Proteomics

journal homepage: www.elsevier.com/locate/euprot

Proteomic comparison of the EWS-FLI1 expressing cells EF with NIH-3T3 and actin remodeling effect of $(R/W)_9$ cell-penetrating peptide

Séverine Clavier[a,b], Françoise Illien[b], Sandrine Sagan[b], Gérard Bolbach[a,b], Emmanuelle Sachon[a,b,*]

[a] Sorbonne Université, UPMC-Univ Paris 6, Ecole Normale Supérieure, PSL Research University, Département de Chimie, CNRS, UMR7203 Laboratoire des BioMolécules, 4 Place Jussieu, Paris Cedex 05, 75252 Paris, France
[b] Sorbonne Université, UPMC—Univ Paris 6, Plateforme de Spectrométrie de Masse et Protéomique-IBPS, cc41, 7-9 Quai Saint Bernard, Paris Cedex 05, 75252 Paris, France

ARTICLE INFO

Article history:
Received 1 June 2015
Received in revised form 25 August 2015
Accepted 25 October 2015
Available online 30 October 2015

Keywords:
EWS-FLI1
Actin cytoskeleton remodeling
Passive dissemination
Cell-penetrating peptide
SILAC quantitative proteomic approach

ABSTRACT

EWS-FLI1 expression in NIH-3T3 fibroblasts has a profound impact on the phenotype, resulting in the cytoskeleton and adhesive capacity disorganization (EF cells). Besides this, $(R/W)_9$, a cell-penetrating peptide (CPP), has an intrinsic actin remodeling activity in EF cells. To evaluate the impact of the oncogenic protein EWS-FLI1 on proteins expression levels, a quantitative comparison of tumoral EF and non-tumoral 3T3 proteomes was performed. Then to see if we could link the EWS-FLI1 oncogenic transformation to the phenotype reversion induced by $(R/W)_9$, $(R/W)_9$ influence on EF cells proteome was assessed. To our knowledge no such "CPPomic" study has been performed before.

Biological significance: Up to now very few global quantitative proteomic studies have been published to help understand the oncogenic transformation induced by EWS-FLI1 fusion protein and leading to Ewing sarcoma development and dissemination. The comparison we did in this study between a model tumoral cell line EF and its non-tumoral counterpart (3T3) allowed us to highlight several features either common to most tumor types or specific to Ewing sarcoma. Particularly, lack of actin cytoskeleton organization could very likely be explained by the down-regulation of many important actin binding proteins. These results are in accordance with the hypothesis of a passive/stochastic mode of dissemination conferring Ewing sarcoma tumoral cell a high metastatic potential.

1. Introduction

Ewing tumors, first described by James Ewing in 1921 [1], are the second most frequent tumor type and are generally developing around or in bones but can also affect soft tissues (extra-osseous Ewing sarcoma). James Ewing first suggested an epithelial cells origin as Ewing's tumors were showing similarities with angio-endothelial tumors [1]. Other origins were further proposed: hematopoietic cells [2], fibroblastic cells [3] or mesenchymal stem cells [4]. Today, the question of the origin of Ewing sarcoma tumor cells remains open.

Ewing sarcoma presents a remarkable characteristic: its oncogenesis is generally accepted to be initiated by a simple genetic event that is a chromosomal translocation between chromosomes 11 and 22 which fuses the EWS gene of chromosome 22 to the FLI1 gene of chromosome 11. The t(11; 22) chromosomal translocation juxtaposes the 5′ sequences from EWS with the 3′ sequence from a member of the ETS transcription factor family (FLI1 gene in 85% of cases) [5]. Fusion of EWS to FLI1 gene yields an oncoprotein EWS-FLI1. EWS-FLI1 acts as a transcriptional regulator to modulate expression of hundreds to thousands genes [6].

The oncogenic transformation resulting from EWS-FLI1 expression was reproduced in a NIH-3T3 fibroblasts cell line [7]. These NIH-3T3 fibroblasts were stably transformed by the transduction of EWS-FLI1 fusion gene, giving birth to the so-called EF cell line. EWS-FLI1 expression has a profound impact on cell phenotype as it is causing a loss of their cytoskeleton organization and adhesive capacity. Cell cytoskeleton is made of actin micro-filaments, intermediate filaments and microtubules. Actin micro-filaments result from the polymerization of monomeric actin molecules (actin-G) and are called actin-F. The actin cytoskeleton is a highly dynamic assembly regulated by a huge number of actin

* Corresponding author at: Sorbonne Université, UPMC-Univ Paris 6, Ecole Normale Supérieure, PSL Research University, Département de Chimie, CNRS, UMR7203 Laboratoire des BioMolécules, 4 Place Jussieu, Paris Cedex 05, 75252 Paris, France.
E-mail address: emmanuelle.sachon@upmc.fr (E. Sachon).

http://dx.doi.org/10.1016/j.euprot.2015.10.002

binding proteins (ABP). Up to now about 150 proteins have been shown to have an actin binding domain and to be able to influence its polymerization state [8]. The different classes of proteins involved in the regulation of actin polymerization include actin monomer sequestration proteins [9] such as thymosin β4 and profilin, nucleation proteins such as Arp2/3 and WASP family [10,11], capping proteins such as gelsolin [12] as well as filament depolymerizing or, on the contrary, filament stabilizing proteins such as tropomyosin or caldesmon [13,14].

As a result of their actin cytoskeleton disorganization, EF cells display small, round cell morphology. The striking loss of actin stress fibers and focal adhesion prevent the formation of protrusions (filapodia, invadopodia . . .) commonly used for the spreading of tumoral cells [15–17]. This lead Chaturvedi et al. to the hypothesis that, contrary to most tumoral cells, cells expressing EWS-FLI1 may disseminate *via* a "passive/stochastic" model [18]. This original behavior and phenotype of Ewing sarcoma tumoral cells is however not yet well characterized at the proteome level.

It was particularly interesting to perform this proteome study as a previous study reported that $(R/W)_9$, a polycationic and amphiphilic cell-penetrating peptide (CPP) of sequence NH_2-RRWWRRWRR-$CONH_2$ (amidated at the C-terminus), able to internalize ubiquitously in eukaryotic cells, displays actin remodeling activity in EF cells [19]. After a few hours of incubation with $(R/W)_9$ peptide, a change in EF cells morphology (already visible using an optical microscope) and a significant reappearance of stress fibers were indeed observed by immunofluorescence. In addition, a decrease in EF cells motility was observed by videomicroscopy. Finally, the ability of EF tumoral cells to grow without anchorage was also shown to be impaired in the presence of the peptide. These results indicate a possible reversion of the EF cells tumoral phenotype in the presence of $(R/W)_9$ CPP [19].

To help filling the gap in proteomic data for Ewing sarcoma and to progress in the understanding of $(R/W)_9$ mode of action on EF tumoral cells, we performed two sets of quantitative differential proteomic experiments. First, we compared tumoral EF and non-tumoral 3T3 cells to see how the oncogenic protein EWS-FLI1 was affecting proteins expression levels. Then to see if, in terms of protein expression, we could link the EWS-FLI1 oncogenic transformation to the phenotype reversion induced by $(R/W)_9$ CPP, we assessed $(R/W)_9$ influence on EF cells proteome.

The comparisons between EF and 3T3 cells proteomes and between EF cells treated by $(R/W)_9$ and untreated EF cells were performed using a robust global differential proteomic strategy based on SILAC quantification technique [20]. One should notice here, that the CPP $(R/W)_9$ used in the work of Delaroche et al. (NH_2-RRWWRRWRR-$CONH_2$) was slightly modified in the present study to incorporate a benzophenone moiety: Biot(O_2)-G_5-K(pBz)-RRWWRRWRR-$CONH_2$ and therefore renamed photo$(R/W)_9$. The photoactivable benzophenone should allow complementary studies such as the search of CPP interacting partners. The biotin should help purification of these partners. Both the biotin tag and the photoactivable probe will not be of interest for the present work but these modifications have required a biological validation to ensure that photo$(R/W)_9$ behaved similarly to $(R/W)_9$, in particular regarding the actin remodeling activity.

2. Experimental

2.1. Photo$(R/W)_9$ peptide synthesis and biological validation

2.1.1. Peptide synthesis

Biot(O_2)-G_5-K(pBz)-RRWWRRWRR-$CONH_2$ (photo$(R/W)_9$) was automatically synthesized (Fmoc strategy) as previously published [21] with some modifications. Briefly, the biologically active $(R/W)_9$ peptide sequence NH_2-RRWWRRWRR-$CONH_2$ was first synthesized with a peptide synthesizer (Applied Biosystems, Darmstadt, Germany, model 433A) using a solid phase butyloxicarbonyl (Boc) chemistry in the 0.1 mmol scale, starting from a *p*-methylbenzhydrylamine resin (MBHA resin). Standard protocols were used, with DCC/HOBt activation (10 eq. excess for standard Boc amino acids). After the removal of the last Nα-Boc protecting group, the synthesis was manually completed by adding the protected Lysine residue (Boc-Lys(Fmoc)-OH). The resin was dried *in vacuo* and separated into two batches for the manual addition of the 5 Boc-Gly-OH followed by the addition of the biotinyl sulfone group. This biotin is oxidized to biotin sulfone (biot(O_2)) to avoid further oxidation during the sample preparation which would dilute the MS signal (more species with lower intensity each). The biotin moiety is separated from the $(R/W)_9$ sequence *via* a string of 5 Gly to ensure flexibility of the spacer arm. The Lysine(Boc-Arg(Tosyl)-OH) and tryptophan (Boc-Trp(Formyl)-OH) residues were then deprotected using 20% piperidin. Then, the carboxybenzophenone was coupled to the lateral chain of the deprotected lysine residue. Finally, both peptidyl-MBHA-resins were treated with liquid HF at 0 °C (2h30) under stirring, in the presence of anisole and dimethylsulfide. After evaporation of HF and of the solvents *in vacuo*, the resins were washed three times with Et_2O and then subsequently extracted three times with 10% AcOH. Lyophilization of the extracts gave crude peptides, which were purified by HPLC and purity was checked by UV (> 95%) and by MALDI-TOF MS.

2.1.2. Cytotoxicity evaluation

The cytotoxicity of photo$(R/W)_9$ for EF cells was tested with a cell counting kit (CCK-8) commercialized by Dojindo (Dojindo Laboratories, Kumamoto, Japan). 20,000 cells were harvested in a 96 wells plate 24 h before the beginning of the peptide treatment. Cells were incubated with photo$(R/W)_9$ or $(R/W)_9$ with concentrations range from 1 to 30 μM. The percentage of cell viability is directly related to the absorbance at 450 nm (Fluostar optima microplate reader, BMG labtech, Offenburg, Germany) of the WST-8 formazan solution and was evaluated after 2 h, 3h30 and 5 h incubation with peptides. Triplicates were performed for each condition (concentration and type of peptide), which were repeated independently at least twice.

2.1.3. Internalization measurements

After a 75 min incubation at 37 °C with a extracellular concentration of 5 or 7.5 μM, internalization capacity of photo $(R/W)_9$ was quantified with a mass spectrometry quantification protocol using the deuterated version of the photo$(R/W)_9$ as the internal standard as previously described [22].

2.1.4. Biological activity

The actin remodeling activity of photo$(R/W)_9$ was assessed by immunofluorescence as previously described [19]. 10,000 cells were harvested on thin 12 mm glass slides coated with gelatin 24 h before treatment with the peptide. These cells were submitted to a 16 h incubation with 5 μM photo$(R/W)_9$. Cells were then washed with PBS, fixed with paraformaldehyde 3%, permeabilized with Triton X-100 0.4% and incubated with phalloïdin FITC and DAPI to label actin stress fibers and cell nuclei (chromatin) respectively. Cells were observed using fluorescence microscopy (Eclipse, TE2000-S, Nikon, Tokyo, Japan).

2.2. 3T3 and EF cell line production

3T3 cells are embryonic mouse fibroblasts. EF cells correspond to a monoclonal cell line obtained by transfection of 3T3 by the cDNA encoding the protein EWS-FLI1 under the influence of the LTR internal promoter of the murine leukemia Moloney virus in a retroviral vector p-BABE-puro containing EWS-FLI1 cDNA and a

puromycin resistant gene allowing for the selection of the transformed cells. The cell line NIH 3T3 transformed by the EWS-FLI1 oncoprotein (EF cells) as well as the corresponding control cell line transfected with an empty vector (3T3 cells) have been provided by Dr. J. Ghysdaël (Institut Curie/CNRS UMR 3306/INSERM U1005).

3T3 and EF cells were cultured in Dulbecco's modified Eagle's medium supplemented with 10% newborn calf serum (Invitrogen), penicillin (100,000 IU/l), and streptomycin (100,000 IU/l) (PAA Laboratories) and selected with 25 μg/ml puromycin (Sigma).

2.3. Stable isotope labeling with amino acids in cell culture (SILAC)

EF and 3T3 cells were grown in A14431-DMEM (high glucose, no glutamine, no lysine, no arginine) media with 10% dialyzed NCS (new-born calf serum), 1% penicillin-streptomycin, 4 mM glutamine and either 146 mg/l L-lysine-2HCl and 84 mg/l L-arginine-HCl, or 146 mg/l $^{13}C_6$ L-lysine-2HCl and 84 mg/l $^{13}C_6{}^{15}N_4$ L-arginine-HCl for six passages, and incorporation efficiency was determined by mass spectrometric analysis. All cultures materials were from Life Technologies and amino-acids (isotopically labeled or not) were from Pierce (Both Thermo Fisher Scientific brands, Waltham, MA, USA).

2.4. Sample preparation

Cells were grown in 10 cm plates making sure that the two cell populations were at the same density and that both were at about 80% confluence on the sample preparation day. EF cells treatment with photo$(R/W)_9$ CPP was performed during the night preceding the sample preparation adding 25 μl of a 1 mM solution of photo $(R/W)_9$ CPP in order to have a 5 μM final concentration in the 5 ml of culture medium. Cells were washed, trypsinized, counted (glasstic slide 10 with grids, Hycor Biomedical, Indianapolis, IN, USA) and mixed at a ratio of 1:1 (2.10^6 cells of each condition). Cells were washed, spinned down and lysed using 100 μl of lysis buffer (100 mM Tris–HCl, 100 mM DTT, 4% SDS). Protein concentration was measured using a BCA assay from Pierce. 100 μg of proteins were separated by 1D-SDS polyacrylamide gel electrophoresis (10%) and stained with Coomassie blue. The gel was sliced into 10 gel bands *prior* to reduction, alkylation and overnight trypsin digestion at 37 °C (1:30 (w:w) protease-to-protein ratio).

2.5. Nano LC–ESI–MS/MS analysis

Protein digests were analyzed by nano-LC (Ultimate 3000, Dionex,Thermo Fisher Scientific) coupled to an ESI-LTQ-Orbitrap (LTQ Orbitrap XL, Thermo Scientific, Bremen, Germany) mass spectrometer. Tryptic peptides were injected by the autosampler and concentrated on a trapping column (Pepmap, C_{18}, 300 μm × 5 mm, 5 μm, 100 Å, Dionex) with water containing 2% acetonitrile (ACN) and 0.1% formic acid (solvent A). After 10 min, the peptides were eluted onto the separation column (Pepmap, C_{18}, 75 μm × 500 mm, 2 μm 100 Å, Dionex) equilibrated with 98% solvent A. Peptides were separated with a gradient 0–50 min 2–40% solvent B (98% ACN + 0.1% formic acid), 50–60 min 40–60% solvent B, and 60–70 min 60% solvent B at a flow rate of 200 nl/min. The LTQ-Orbitrap mass spectrometer is outfitted with a nano ESI interface. Electrospray emitters were 360/20 μm o.d. × 10 μm i.d. fused-silica tips (PicoTip Emitter, Standard Coated SilicaTip, New Objective, Woburn, MA, USA). The heated capillary temperature and spray voltage were 200 °C and 1.5 kV, respectively. Orbitrap spectra (automated gain control (AGC) 2.10^5) were collected from *m*/*z* 500–2000 at a resolution of 30,000 in the profile mode followed by data dependent sequential CID MS/MS spectra of the ten most intense ions with a normalized energy of 35. A dynamic exclusion time of 60 s was used to discriminate against previously analyzed ions.

2.6. Data treatment, statistical analysis and interpretation

The peptides were identified and quantified using the Proteome Discoverer 1.3 software (Thermo Scientific) with carbamidomethylation (C), oxidation (M), $^{13}C_6$ (K) and $^{13}C_6{}^{15}N_4$ (R) as variable modifications. The database used for protein identification is the Uniprot protein database for the taxonomy *Mus musculus* (downloaded on http://www.uniprot.org/, 30th October 2013, 74,249 entries). False Discovery Rate (FDR) calculated at the peptide level with a decoy database (reversed peptides sequences) was set to 1%, MS tolerance was 10 ppm and MS/MS tolerance was 0.8 Da. Protein ratios were corrected using the median protein ratio normalization.

The statistical analysis of the proteins lists obtained for each experiment was performed with MyProMS software [23]. The threshold values for absolute fold change in protein expression and p-value for the ratio calculation were determined with a control experiment mixing identical EF cells grown in light and heavy medium at a ratio of 1:1. Proteins were found to be significantly over- or under-expressed from an absolute fold change of 1.3 and a p-value < 0.05. Three biological replicates of the experiment comparing (1) EF *versus* 3T3 and (2) EF treated with photo $(R/W)_9$ *versus* EF untreated were performed.

Only proteins with a ratio corresponding to a fold change greater than 1.5, with a p-value < 0.05 and quantified in at least two of the three replicates with at least two peptides were kept for data interpretation.

Analysis of the protein networks for significantly over- or under-expressed proteins was performed using the STRING software available online (http://string-db.org/) [24,25].

3. Results and discussion

3.1. Biological validation of the actin remodeling activity of photo$(R/W)_9$ peptide in tumoral EF cells

Cytotoxicity assays with photo$(R/W)_9$ on EF cells have shown that this CPP affects the cell viability above 7.5 μM extracellular concentration (Fig. S1-A). Photo$(R/W)_9$ is more cytotoxic than $(R/W)_9$ for which no cell viability decrease was observed until 30 μM (not shown)[19]. However it should be noted that this higher cytotoxicity can very likely be explained by a much higher internalization capacity, about six times more efficient for photo $(R/W)_9$ compared to $(R/W)_9$ (≈3 pmol *versus* ≈0.5 pmol, respectively at 5 μM extracellular concentration) (Fig. S1-B). For the comparison of EF cells treated with photo$(R/W)_9$ CPP untreated EF cells, a 5 μM extracellular concentration was further used to prevent any cytotoxicity effect. (For photo$(R/W)_9$ this corresponds to about 2.10^6 CPP molecules internalized in each cell, taking into account an estimated cell volume of 1.5 pl [22]). Finally immunofluorescence experiments indicated that the addition of the photoprobe and the biotin tag to the $(R/W)_9$ sequence did not affect its actin remodeling activity. Photo$(R/W)_9$ thus proved to be a suitable model to investigate the actin remodeling effect previously observed for $(R/W)_9$ [19] (Fig. S2).

3.2. Comparison of tumoral (EF) and non-tumoral (3T3) cell proteomes, using a SILAC experiment

EF cells have been labeled with heavy Arg and Lys whereas 3T3 cells were grown with light amino-acids. Quantification of the protein levels (heavy/light) was done using the software Proteome Discoverer 1.3 (Thermo Fisher Scientific) (Supplemental file S9)

and the statistical analysis of the lists of under- or over-expressed proteins obtained for each quantification experiment was performed using MyProMS software [23]. Based on the filtering criteria determined with control experiments (fold change >1.5, *p*-value < 0.05 and presence in at least two of the three replicates experiments) we were able to obtain a list of 94 proteins (among 1700 proteins quantified) with a significant variation of expression level between EF and 3T3. Among these 94 proteins, 43 were over-expressed and 51 under-expressed in EF compared to 3T3. The volcano plot obtained for the comparison of EF *versus* 3T3 proteome is presented in Fig. 1 while the lists of proteins with significantly modified expression levels are presented in Fig. 3-A and -B.

These differences are compiled in Fig. 2 which summarizes the results obtained and described in details in the following paragraphs. The common features of tumoral cells are highlighted as well as features specific to Ewing sarcoma tumors.

3.3. Proteins significantly over-expressed in EF cells compared to 3T3 cells

3.3.1. Glycolysis increase

For the upregulated proteins network, the most densely populated interaction node corresponds to proteins involved in glycolytic processes (Fig. S4).

This increase of glycolysis is a quasi-universal property for primary tumor or metastatic cells [26,27]. Actually, in addition to the ATP necessary for homeostatic cell activity, cancer cells need supplemental energy to sustain their rapid growth. Moreover it has been shown that tumoral cells, instead of producing ATP *via* a classical aerobic and efficient two-steps process involving glycolysis and the Krebs cycle (36 ATP molecules produced per glucose molecule), are performing anaerobic glycolysis (10 ATP molecules produced per glucose molecule). This metabolic phenotype is known as the Warburg effect [28].

Therefore, to compensate this energy loss and to ensure a greater and faster ATP production, tumoral cells have to consume a larger quantity of glucose, which explains the up-regulation of several proteins involved in the glycolysis process.

3.3.2. Increase of biosynthetic processes

Among the 43 significantly up-regulated proteins (Fig. S3-A), 13 are directly involved in biosynthetic processes (monosaccharides, nucleotides, amino acids biosynthesis pathways . . .) (Fig. S5). Tumoral cells which are characterized by a greater growth rate actually need more “building blocks” to sustain their proliferation [29]. Increase in biosynthetic processes requiring high amount of energy is thus directly linked with the increased glycolysis.

3.3.3. Oncogenic proteins

One can also notice the up-regulation of proteins known to be involved in oncogenic processes such as moesin whose over-expression was found necessary to the epithelial-mesenchymal transition (EMT) of tumoral cells leading to metastasis formation [30]. Another example is the insulin like growth factor 2 (IGF-2), a mitogenic peptide of 7.5 kDa over-expressed in several cancers and generally associated with a poor diagnosis [31,32] .The proliferating cell nuclear antigen (PCNA) which is a marker of cell proliferation [33] and the Y-box protein 1 also known as nuclease-sensitive element-binding protein 1, a marker of tumor aggressiveness [34] are also interesting markers to distinguish tumoral EF from non-tumoral 3T3 cells.

3.3.4. Up-regulation of an actin stress fiber dissoluting protein

The protein STE20 like serine/threonine protein kinase (SLK) plays a role in remodeling of actin cytoskeleton [35]. It was shown

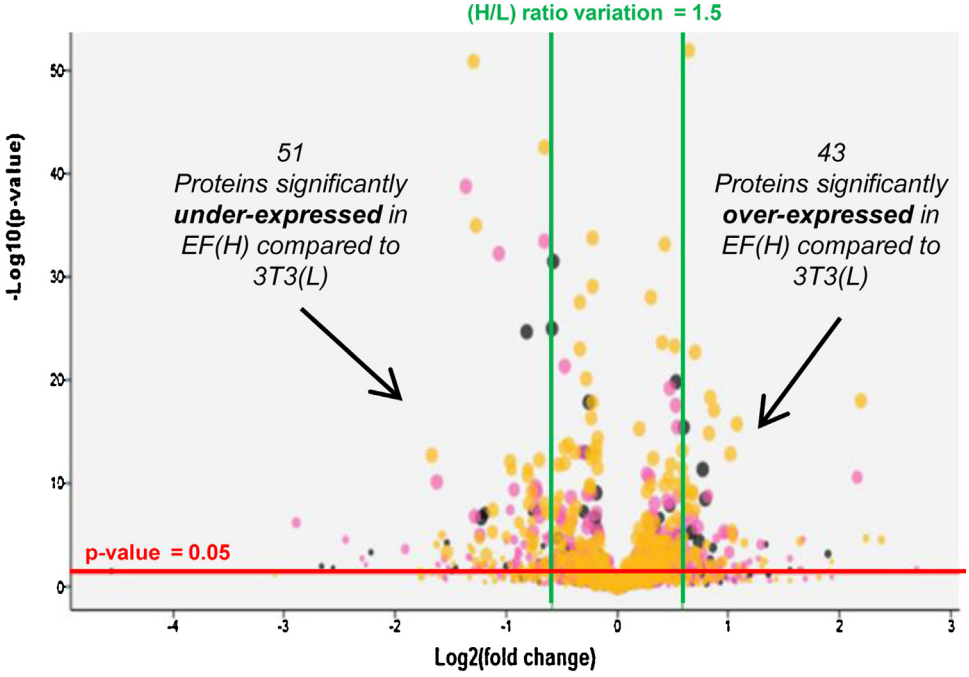

Fig. 1. Volcano plot obtained using MyProMS software [21] for the comparison of tumoral cells EF (heavy = H) and their non-tumoral counterparts 3T3 (light = L). Each spot corresponds to a protein. The three colours, orange, pink and black are referring to the three biological replicates. (H) and (L) indicate that the cells have been grown with heavy labelled amino acids ($^{13}C_6{}^{15}N_4$ L-arginine and $^{13}C_6$ L-lysine) or classical amino acids, respectively. The x axis corresponds to the H/Lratio of quantified proteins in $\log_2$ scale while the y axis corresponds to the *p*-value for the protein H/L ratio determined using the different H/L peptides ratios for this protein. Vertical green lines correspond to the 1.5 fold change in protein expression level. The horizontal red line corresponds to a *p*-value = 0.05. These threshold values have been determined with control experiments (not shown) for which no protein was found with a *p*-value < 0.05 and a fold change above 1.3. Outside the zone delimited by these lines are proteins with a significantly modified expression between EF and 3T3 cells: on the left are proteins under-expressed in tumoral EF cells and on the right the over-expressed ones.

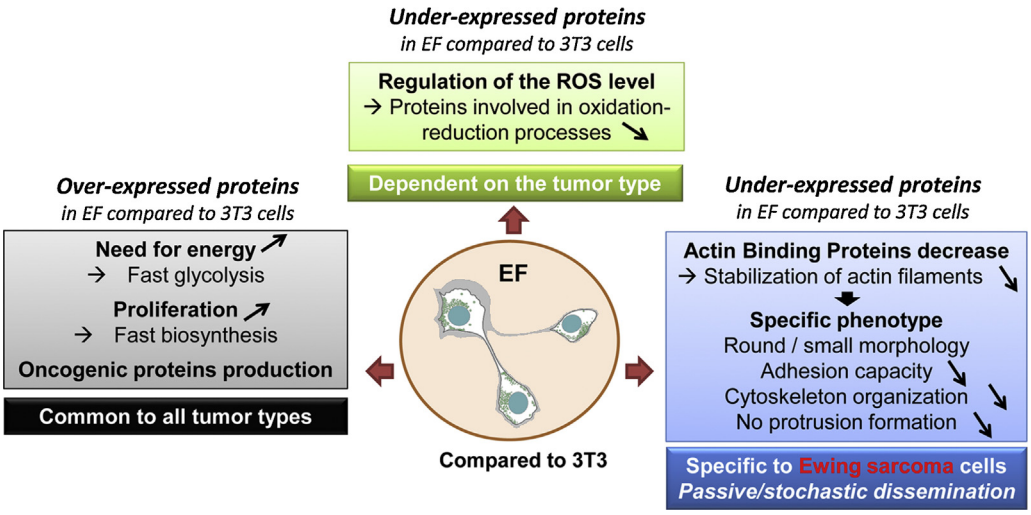

Fig. 2. Scheme summarizing key features of EF cells (an Ewing sarcoma model cell line) evidenced by proteins expression level variations existing between tumoral EF and non-tumoral 3T3 cells. These features are either common to other tumor types or specific to Ewing sarcoma cells.

that over-expression of this protein causes the retraction of cells from their substrate and thus inhibits their active migration along this surface. This decreased adhesion is likely due to the dissolution of actin stress fibers by SLK [36]. The SLK over-expression observed in EF compared to 3T3 is thus in good agreement with the "passive/stochastic" way of dissemination of cells expressing EWS-FLI-1 described by Chaturvedi [18].

3.4. Proteins significantly under-expressed in EF cells compared to 3T3 cells

3.4.1. Decrease of the oxidation-reduction and respiration processes

Among the 51 under-expressed proteins, 11 are directly involved in oxidation-reduction processes (Fig. S6). Tumoral cells compared to normal cells are under oxidative stress conditions due to an increased metabolic activity neglecting mitochondria and respiration processes [37], as already described in the previous section. This oxidative stress is characterized by an increased level of reactive oxygen species (ROS). ROS include free radicals such as superoxides ($O_2^{\bullet}$), hydroxyl radicals ($HO^{\bullet}$) as well as non-radical molecules such as H_2O_2.

It was shown that this increase in ROS level could have numerous beneficial consequences for the tumoral cells. Actually it appears that ROS stimulate cell proliferation and contribute to mutations and genetic instabilities responsible for cancer drug treatment resistance [38]. However, the mechanisms resulting in oxidative stress observed in numerous cancers are not yet precisely understood. It is especially difficult to assess the threshold of ROS concentration necessary to maintain a favorable situation for tumoral proliferation and one threatening cell survival.

Expression level modifications of proteins involved in oxidation-reduction processes are a common feature for tumoral cells. [Cu–Zn] and [Mn] superoxide dismutases (SOD), glutathione-S-transferase Mu1 and Mu2, cytoplasmic and mitochondrial NADPH isocitrate deshydrogenases or peroxiredoxin-2 are proteins with anti-oxidants properties we identified with significantly decreased expression levels in EF cells (Fig. S3-B). In a majority of cancers, expression levels of antioxidant proteins such as SODs are rather increased, likely to prevent cells from reaching a cytotoxic concentration of ROS [39,40]. However in other types of cancer, expression levels of SOD are decreased [41,42] as we observed herein. This suggests that the way cancer cells regulate their ROS level is varying from one cell type to another, and that in Ewing sarcoma the level of ROS necessary to preserve the cancer cells is reached by decreasing the expression level of proteins with anti-oxidant properties.

On the contrary, it is interesting to notice that the hypoxia up-regulated protein 1 is significantly over-expressed in EF cells compared to 3T3 indicating that EF cells are under hypoxic conditions. Several studies [26,43] have shown that tumoral cells can adapt to low oxygen conditions, a situation they have to face to develop in invaded tissues before the setup of new blood vessels (angiogenesis).

3.4.2. Down-regulation of actin binding proteins

Actin cytoskeleton has a fundamental role in the cell life and cycle (cell division, migration, signals transmission . . .) and mechanisms regulating actin dynamics rely on a large number of actin binding proteins. The expression levels of these proteins are usually modified during oncogenesis [44,45]. However to our knowledge, these modifications in actin binding protein levels have not yet been described in details in the literature for the oncogenic transformation caused by EWS-FLI1.

A careful analysis of the list of under-expressed proteins (Fig. S3-B) allowed us to identify a total of 12 proteins known to be involved in actin dynamics. These proteins are gathered in Table 1 as well as their expression level variations and biological processes implications [13,14,46–52].

With the exception of destrin and gelsolin contributing to the maintenance of a monomeric actin pool [48,50], all the other actin binding proteins identified with decreased expression levels in EF cells compared to 3T3 play a role in the stabilization of actin filaments (tropomyosin, caldesmon) [13,14], in their assembly into network or bundles (filamin, prelamin A/C, lamin B1, myosin II subunit, calponin-3) [47,49,51,52] or in the membrane adhesion (LASP-1) [46].

Most of these proteins are linked to "actin filament based process" gene ontology (GO) term [53] that is significantly enriched for this list of proteins as depicted in Fig. 3.

Consequently this comparison of tumoral EF with non-tumoral 3T3 cells indicates that the oncogenic transformation induced by the presence of the fusion protein EWS-FLI1 is leading to a significant decrease of several key actin binding proteins. This result is against what is currently seen for tumoral cells which tend to reinforce their actin network in order to disseminate by migration *via* the formation of filipodia, lamellipodia, *etc.* [15–17]. Nonetheless, this conclusion is in good agreement with Chaturvedi et *al.* study [3] who have evidenced an original behavior of Ewing

Table 1
List of actin binding proteins (ABP) identified among the list of proteins under-expressed in tumoral EF (H) cells compared to non-tumoral 3T3 (L) cells. The second column indicates the average H/L ratio and the associated coefficient of variation (CV in percentage) obtained for the three biological replicates (Figure S7 gives details about the different H/L values obtained). The third column describes the function of these proteins on actin cytoskeleton dynamics.

Actin binding proteins (ABP's)	Average H/L ratio and associated CV	Function	References
LIM and SH3 domain protein 1 (LASP-1)	1/1.9 (±4%)	Regulation of cellular functions associated with actin cytoskeleton reorganization at the membrane. Part of focal adhesion points and associated with zyxin	[46]
Filamin (Flna)	1/2.1 (±16%)	Actin filaments cross-linking and orthogonal actin networks building blocks	[47]
Destrin (Dstn) (or Actin depolymerizing factor ADF)	1/2.1 (±15%)	Sequestration of actin filaments and binding to actin monomers	[48]
Prelamin A/C	1/2.4 (±5%)	Role in actin bundling	[49]
Lamin B1	1/1.5 (±4%)	Role in actin bundling	[49]
Gelsolin (Gsn)	1/2.6 (±18%)	Actin filaments capping and monomers sequestration	[50]
Myosin (myosin regulatory light chain 12B (Myl12b) + myosin-9 (Myh9) + myosin light polypeptide 6 (My16))	1/1.5 (±7%) 1/1.5 (±4%) 1/1.5 (±3%)	Part of Myosin II complex linked to actin and pivotal role in cellular adhesion, migration and division. Down-regulation of myosin regulatory light chains A or B (MYL12B/12A) induces important cell morphology changes and disappearance of actin stress fibers	[51]
Tropomyosin	1/1.5 (±15%)	Lateral stabilization of actin filaments	[13]
Caldesmon (Cald1)	1/1.9 (±24%)	Lateral stabilization of actin filaments	[14]
Calponin-3 (Cnn-3)	1/2.2 (±22%)	Role in actin stress fibers formation	[52]

sarcoma cells with a passive/stochastic dissemination rather than an active migration. Thus, EF cell phenotype characterized by a disorganized actin cytoskeleton lacking stress fibers, by a round morphology and the absence of focal adhesion point appears to result from the down-regulation of several key actin binding proteins as the ones we identified in this study.

3.5. Assessment of photo(R/W)$_9$ treatment on EF cells proteome

As previously mentioned in the introduction section, the cell-penetrating peptide (CPP) (R/W)$_9$ has been reported [19] to reverse the tumoral phenotype of the EF cells to 3T3 non-tumoral-like phenotype with the reappearance of actin stress fibers in EF cells after a few hours incubation with this CPP. In order to examine whether we can correlate the proteomic differences found between EF and 3T3 cells with the phenotype changes observed by immunofluorescence, we compared the proteome of EF cells grown in a light medium treated overnight with photo(R/W)$_9$ (5 μM) to the one of untreated EF cells grown with heavy Arg and Lys medium.

As for the comparison of EF *versus* 3T3 cells, three biological replicates were studied to assess the effect of photo(R/W)$_9$ CPP on the EF cells proteome (Supplemental file S10). Again the threshold values for the absolute fold change and *p*-value determined in the control experiment were used. However in this case, among the 1745 proteins identified (1% FDR) and quantified (2 peptides minimum), none was found with an expression level significantly and reproducibly modified (Fig. S8).

Therefore, the strong phenotype change of EF cells observed by immunofluorescence (Fig. S2) and also simply with an optical

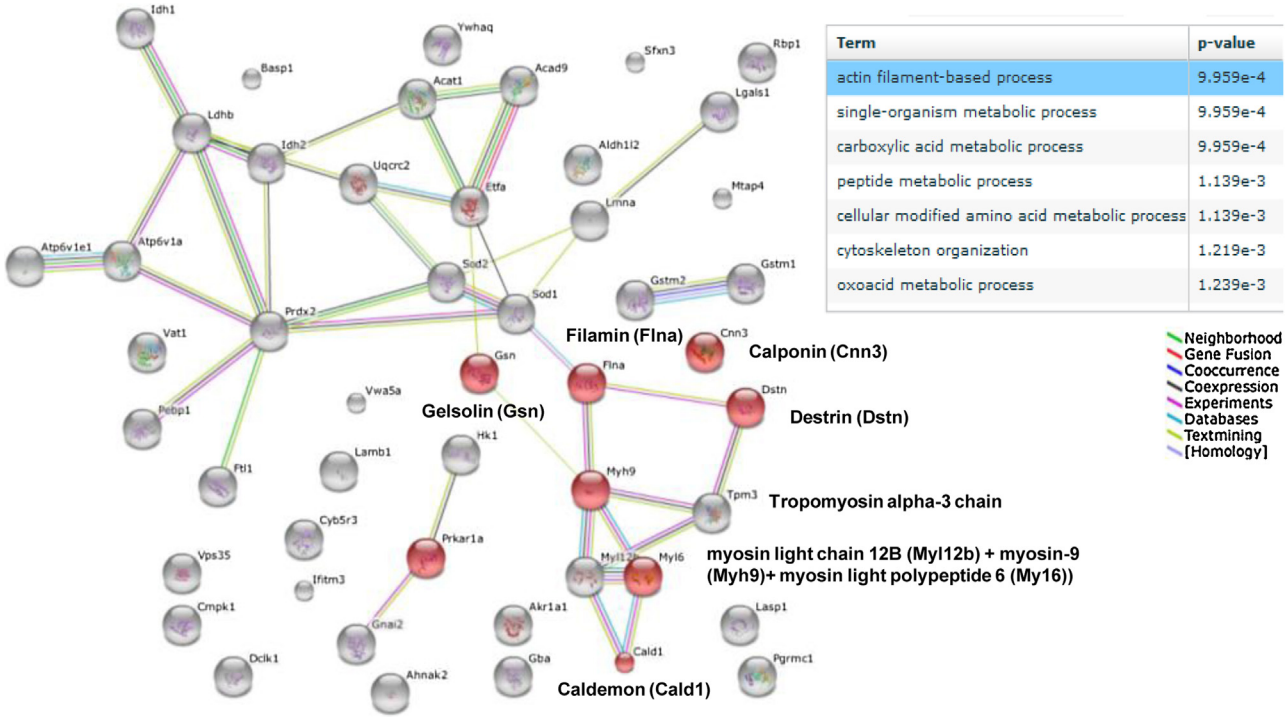

Fig. 3. Interaction network generated with the list of significantly over-expressed proteins in EF *versus* T3 using the open source STRING software [24,25]. Spheres coloured in red are corresponding to proteins known to be involved in actin dynamics and gathered under the actin filament-based process GO term which is one of the mostly enriched term in this list (*p*-value ≈ 1.10^{-3}).

microscope after 18 h treatment with photo(R/W)$_9$ peptide, does not result from important modifications of the EF cell proteome.

In SILAC based quantitative proteomic experiments we have access to the relative expression levels quantification for a significant part of the cell proteins. However one should keep in mind that even with efforts made in the fractionation of the cell lysates as well as in the MS analysis we are still limited in the number of proteins we are able to identify, notably because of the great dynamic range of protein expression levels. Consequently we are mostly looking at the proteins produced in large quantities by the cells. In addition, even with isotope labeling, systematic error in peptide relative quantification due to biology variability led us to only consider important expression changes (>1.5 fold change). The energetic cost for cells to increase the production of an abundant protein by 50% can be more important than the one to double or triple the quantity of less abundant proteins. Unfortunately these weakly abundant proteins remain difficult to detect in global proteomic approaches. Beyond these limitations of protein abundance and range of expression variations, it has been demonstrated that PTMs are crucial and can quickly boost a protein activity [54] at constant expression level and may even compensate a decrease in expression level. Consequently an in depth study of PTMs such as phosphorylation might help understanding photo(R/W)$_9$ mode of action.

Another important option to consider in order to explain phenotype changes at constant protein levels is protein organization in the cells. Protein-protein interactions play a key role in regulating signaling pathways and thus cellular functions. At 5 μM extracellular concentration about 2.10^6 photo(R/W)$_9$ molecules are internalized per cell. Although the number of photo(R/W)$_9$ molecules internalized is about two orders of magnitude lower than the number of actin monomers (estimated to be 5.10^8 molecules per cell) [56], photo(R/W)$_9$ CPP molecules could disrupt some actin related protein complexes or stabilize others. The presence of photo(R/W)$_9$ molecules could thus compensate the down-regulation of key actin binding proteins evidenced in EF *versus* 3T3 and lead to actin stress fibers formation through direct interaction with actin [55] and to subsequent morphological changes.

4. Conclusions

The gap between genome and phenotype has been evidenced already a while ago and proteomics was shown to be an extremely useful tool to help filling this gap [56]. The quantitative proteomic experiments realized to compare tumoral EF and non-tumoral 3T3 actually help us to gain insight in the molecular changes drove by EWS-FLI1 oncogene and offer a set of proteomic data to biologists working on Ewing sarcoma. We can already say from these data that EF cells expressing EWS-FLI1 protein exhibit some characteristic features of tumoral cell at the proteome level such as metabolic changes (bioenergetics, biosynthesis, redox status). In addition, the down-regulation of several key actin-binding proteins distinguishes Ewing sarcoma cells from the great majority of tumoral cells and is here proposed to explain the peculiar phenotype of EF cells as well as their particular mode of dissemination.

The second objective of the study, that was to understand the photo(R/W)$_9$ mode of action on EF cells, revealed that a phenotype change can not necessarily easily be seen using a global quantitative proteomic approach. Moreover this study indicates that even if proteomics has allowed a big step forward in the correlation between a molecular perturbation and the associated phenotype it is still not straightforward to link a phenotype change and proteome. Especially, with these experiments we saw that similar phenotypes can correspond to clearly different proteomes and that a drastic phenotype change is not necessarily related to important changes in proteins expression levels.

Conflict of interest

None.

Associated content

Supporting Information Available: eight additional figures (S1–S8) are presented in the electronic supplementary material. Excel spreadsheets exported from P.D 1.3 software and containing the identification and quantification data for EF comparison with 3T3 (3 biological replicates) and for EF treated by photo(R/W)$_9$ comparison with untreated EF (3 biological replicates) are also provided (S9 and S10).

Acknowledgements

The authors wish to thank J. Ghysdaël for the kind gift of EF and 3T3 cell lines, R. Marquant for peptide synthesis and purification, as well as P. Poullet and G. Arras who provided their help for MyProMS software installation and training. The authors also thank G. Clodic for help and technical support.

Appendix A. Supplementary data

Supplementary data associated with this article can be found, in the online version, at http://dx.doi.org/10.1016/j.euprot.2015.10.002.

References

[1] J. Ewing, Classics in oncology. Diffuse endothelioma of bone, in: James Ewing (Ed.), Proceedings of the New York Pathological Society, 1921. CA Cancer J. Clin. 22 (1972) 95–98.
[2] M.E. Kadin, K.G. Bensch, On the origin of Ewing's tumor, Cancer 27 (1971) 257–273.
[3] P.S. Dickman, L.A. Liotta, T.J. Triche, Ewing's sarcoma: characterization in established cultures and evidence of its histogenesis, Lab. Investig. J. Tech. Methods Pathol. 47 (1982) 375–382.
[4] J.J. Navas-Palacios, R. Aparicio-Duque, M.D. Valdés, On the histogenesis of Ewing's sarcoma. An ultrastructural, immunohistochemical, and cytochemical study, Cancer 53 (1984) 1882–1901.
[5] O. Delattre, J. Zucman, B. Plougastel, C. Desmaze, T. Melot, M. Peter, et al., Gene fusion with an ETS DNA-binding domain caused by chromosome translocation in human tumours, Nature 359 (1992) 162–165, doi:http://dx.doi.org/10.1038/359162a0.
[6] A. Prieur, F. Tirode, P. Cohen, O. Delattre, EWS/FLI-1 silencing and gene profiling of Ewing cells reveal downstream oncogenic pathways and a crucial role for repression of insulin-like growth factor binding protein 3, Mol. Cell. Biol. 24 (2004) 7275–7283, doi:http://dx.doi.org/10.1128/mcb.24.16.7275-7283.2004.
[7] W.A. May, M.L. Gishizky, S.L. Lessnick, L.B. Lunsford, B.C. Lewis, O. Delattre, et al., Ewing sarcoma 11;22 translocation produces a chimeric transcription factor that requires the DNA-binding domain encoded by FLI1 for transformation, Proc. Natl. Acad. Sci. U. S. A. 90 (1993) 5752–5756.
[8] C.G. Remedios, C. dos, D. hhabra, M. Kekic, I.V. Dedova, M. Tsubakihara, D.A. Berry, et al., Actin binding proteins: regulation of cytoskeletal microfilaments, Physiol. Rev. 83 (2003) 433–473, doi:http://dx.doi.org/10.1152/physrev.00026.2002.
[9] L.G. Tilney, S. Hatano, H. Ishikawa, M.S. Mooseker, The polymerization of actin: its role in the generation of the acrosomal process of certain echinoderm sperm, J. Cell Biol. 59 (1973) 109–126.
[10] M.D. Welch, J. Rosenblatt, J. Skoble, D.A. Portnoy, T.J. Mitchison, Interaction of human Arp2/3 complex and the Listeria monocytogenes ActA protein in actin filament nucleation, Science 281 (1998) 105–108.
[11] R.D. Mullins, J.A. Heuser, T.D. Pollard, The interaction of Arp2/3 complex with actin: nucleation, high affinity pointed end capping, and formation of branching networks of filaments, Proc. Natl. Acad. Sci. U. S. A. 95 (1998) 6181–6186.
[12] J.A. Cooper, T.D. Pollard, Effect of capping protein on the kinetics of actin polymerization, Biochem. (Mosc.) 24 (1985) 793–799.
[13] B.W. Bernstein, J.R. Bamburg, Tropomyosin binding to F-actin protects the F-actin from disassembly by brain actin-depolymerizing factor (ADF), Cell Motil. 2 (1982) 1–8.

[14] S. Marston, D. Burton, O. Copeland, I. Fraser, Y. Gao, J. Hodgkinson, et al., Structural interactions between actin, tropomyosin, caldesmon and calcium binding protein and the regulation of smooth muscle thin filaments, Acta Physiol. Scand. 164 (1998) 401–414.
[15] H. Yamaguchi, J. Condeelis, Regulation of the actin cytoskeleton in cancer cell migration and invasion, Biochim. Biophys. Acta 1773 (2007) 642–652, doi: http://dx.doi.org/10.1016/j.bbamcr.2006.07.001.
[16] P.K. Mattila, P. Lappalainen, Filopodia: molecular architecture and cellular functions, Nat. Rev. Mol. Cell Biol. 9 (2008) 446–454, doi:http://dx.doi.org/10.1038/nrm2406.
[17] A.M. Weaver, Invadopodia: specialized cell structures for cancer invasion, Clin. Exp. Metastasis 23 (2006) 97–105, doi:http://dx.doi.org/10.1007/s10585-006-9014-1.
[18] A. Chaturvedi, L.M. Hoffman, A.L. Welm, S.L. Lessnick, M.C. Beckerle, The EWS/FLI oncogene drives changes in cellular morphology, adhesion, and migration in Ewing sarcoma, Genes Cancer 3 (2012) 102–116, doi:http://dx.doi.org/10.1177/1947601912457024.
[19] D. Delaroche, F.-X. Cantrelle, F. Subra, C. Van Heijenoort, E. Guittet, C.-Y. Jiao, et al., Cell-penetrating peptides with intracellular actin-remodeling activity in malignant fibroblasts, J. Biol. Chem. 285 (2010) 7712–7721, doi:http://dx.doi.org/10.1074/jbc.M109.045872.
[20] S.-E. Ong, B. Blagoev, I. Kratchmarova, D.B. Kristensen, H. Steen, A. Pandey, et al., Stable isotope labeling by amino acids in cell culture, SILAC, as a simple and accurate approach to expression proteomics, Mol. Cell. Prot. MCP 1 (2002) 376–386.
[21] S. Clavier, G. Bolbach, E. Sachon, Photocross-linked peptide-protein complexes analysis: A comparative study of CID and ETD fragmentation modes, J Am Soc Mass Spectrom (2015) 1014–1026, doi:http://dx.doi.org/10.1007/s13361-015-1095-0.
[22] F. Burlina, S. Sagan, G. Bolbach, G. Chassaing, A direct approach to quantification of the cellular uptake of cell-penetrating peptides using MALDI-TOF mass spectrometry, Nat. Protoc. 1 (2006) 200–205, doi:http://dx.doi.org/10.1038/nprot.2006.30.
[23] P. Poullet, S. Carpentier, E. Barillot, myProMS, a web server for management and validation of mass spectrometry-based proteomic data, Proteomics 7 (2007) 2553–2556, doi:http://dx.doi.org/10.1002/pmic.200600784.
[24] D. Szklarczyk, A. Franceschini, M. Kuhn, M. Simonovic, A. Roth, P. Minguez, et al., The STRING database in functional interaction networks of proteins, globally integrated and scored, Nucl. Acids Res. 39 (2011) D561–D568, doi: http://dx.doi.org/10.1093/nar/gkq973.
[25] A. Franceschini, D. Szklarczyk, S. Frankild, M. Kuhn, M. Simonovic, A. Roth, et al., STRING v9. 1: protein–protein interaction networks, with increased coverage and integration, Nucl. Acids Res 41 (2013) D808–D815, doi:http://dx.doi.org/10.1093/nar/gks1094.
[26] R.A. Gatenby, R.J. Gillies, Why do cancers have high aerobic glycolysis? Nat. Rev. Cancer 4 (2004) 891–899, doi:http://dx.doi.org/10.1038/nrc1478.
[27] H. Pelicano, D.S. Martin, R.-H. Xu, P. Huang, Glycolysis inhibition for anticancer treatment, Oncogene 25 (2006) 4633–4646, doi:http://dx.doi.org/10.1038/sj.onc.1209597.
[28] O. Warburg, On the origin of cancer cells, Science 123 (1956) 309–314, doi: http://dx.doi.org/10.1126/science.123.3191.309.
[29] H. Vander, M.G. eiden, S.Y. Lunt, T.L. Dayton, B.P. Fiske, W.J. Israelsen, K.R. Mattaini, et al., Metabolic pathway alterations that support cell proliferation, Cold Spring Harb. Symp. Quant. Biol. 76 (2011) 325–334, doi:http://dx.doi.org/10.1101/sqb.2012.76.010900.
[30] J. Haynes, J. Srivastava, N. Madson, T. Wittmann, D.L. Barber, Dynamic actin remodeling during epithelial-mesenchymal transition depends on increased moesin expression, Mol. Biol. Cell 22 (2011) 4750–4764, doi:http://dx.doi.org/10.1091/mbc.e11-02-0119.
[31] K. Kawamoto, H. Onodera, S. Kondo, S. Kan, D. Ikeuchi, S. Maetani, et al., Expression of insulin-like growth factor-2 can predict the prognosis of human colorectal cancer patients: correlation with tumor progression, proliferative activity and survival, Oncology 55 (1998) 242–248.
[32] H. Yu, T. Rohan, Role of the insulin-like growth factor family in cancer development and progression, J. Natl. Cancer Inst. 92 (2000) 1472–1489.
[33] D. van, P.J. iest, G. Brugal, J.P. Baak, Proliferation markers in tumours: interpretation and clinical value, J. Clin. Pathol. 51 (1998) 716–724.
[34] J. Huang, P.-H. Tan, K.-B. Li, K. Matsumoto, M. Tsujimoto, B.-H. Bay, Y-box binding protein, YB-1, as a marker of tumor aggressiveness and response to adjuvant chemotherapy in breast cancer, Int. J. Oncol. 26 (2005) 607–613.
[35] L.A. Sabourin, K. Tamai, P. Seale, J. Wagner, M.A. Rudnicki, Caspase 3 cleavage of the Ste20-related kinase SLK releases and activates an apoptosis-inducing kinase domain and an actin-disassembling region, Mol. Cell Biol. 20 (2000) 684–696.
[36] S. Wagner, T.A. Flood, P. O'Reilly, K. Hume, L.A. Sabourin, Association of the Ste20-like kinase (SLK) with the microtubule. Role in Rac1-mediated regulation of actin dynamics during cell adhesion and spreading, J. Biol. Chem. 277 (2002) 37685–37692, doi:http://dx.doi.org/10.1074/jbc.m205899200.
[37] V. Gogvadze, B. Zhivotovsky, S. Orrenius, The Warburg effect and mitochondrial stability in cancer cells, Mol. Asp. Med. 31 (2010) 60–74, doi: http://dx.doi.org/10.1016/j.mam.2009.12.004.
[38] H. Pelicano, D. Carney, P. Huang, ROS stress in cancer cells and therapeutic implications, Drug Resist Updat: Rev. Comment Antimicrob. Anticancer Chemother. 7 (2004) 97–110, doi:http://dx.doi.org/10.1016/j.drup.2004.01.004.
[39] A.M. Janssen, C.B. Bosman, L. Kruidenier, G. Griffioen, C.B. Lamers, K. van, J.H. rieken, et al., Superoxide dismutases in the human colorectal cancer sequence, J. Cancer Res. Clin. Oncol. 125 (1999) 327–335.
[40] K. Punnonen, M. Ahotupa, K. Asaishi, M. Hyöty, R. Kudo, R. Punnonen, Antioxidant enzyme activities and oxidative stress in human breast cancer, J. Cancer Res. Clin. Oncol. 120 (1994) 374–377.
[41] L.W. Oberley, I.B. Bize, S.K. Sahu, S.W. Leuthauser, H.E. Gruber, Superoxide dismutase activity of normal murine liver, regenerating liver, and H6 hepatoma, J. Natl. Cancer Inst. 61 (1978) 375–379.
[42] D. Van, B.E. riel, H. Lyon, D.C. Hoogenraad, S. Anten, U. Hansen, N. Van, C.J. oorden, Expression of CuZn- and Mn-superoxide dismutase in human colorectal neoplasms, Free Radic. Biol. Med. 23 (1997) 435–444.
[43] T.G. Graeber, C. Osmanian, T. Jacks, D.E. Housman, C.J. Koch, S.W. Lowe, et al., Hypoxia-mediated selection of cells with diminished apoptotic potential in solid tumours, Nature 379 (1996) 88–91, doi:http://dx.doi.org/10.1038/379088a0.
[44] J.Y. Rao, N. Li, Microfilament actin remodeling as a potential target for cancer drug development, Curr. Cancer Drug Targets 4 (2004) 345–354, doi:http://dx.doi.org/10.2174/1568009043332998.
[45] D.-H. Kim, J. Bae, J.W. Lee, S.-Y. Kim, Y.-H. Kim, J.-Y. Bae, et al., Proteomic analysis of breast cancer tissue reveals upregulation of actin-remodeling proteins and its relevance to cancer invasiveness, Proteom. Clin. Appl. 3 (2009) 30–40, doi:http://dx.doi.org/10.1002/prca.200800167.
[46] H. Zhang, X. Chen, W.B. Bollag, R.J. Bollag, D.J. Sheehan, C.S. Chew, Lasp1 gene disruption is linked to enhanced cell migration and tumor formation, Physiol. Genom. 38 (2009) 372–385, doi:http://dx.doi.org/10.1152/physiolgenomics.00048.2009.
[47] A. van der Flier, A. Sonnenberg, Structural and functional aspects of filamins, Biochim. Biophys. Acta 1538 (2001) 99–117.
[48] Y. Estornes, F. Gay, J.-C. Gevrey, S. Navoizat, M. Nejjari, J.-Y. Scoazec, et al., Differential involvement of destrin and cofilin-1 in the control of invasive properties of Isreco1 human colon cancer cells, Int. J. Cancer 121 (2007) 2162–2171, doi:http://dx.doi.org/10.1002/ijc.22911.
[49] D.N. Simon, M.S. Zastrow, K.L. Wilson, Direct actin binding to A- and B-type lamin tails and actin filament bundling by the lamin A tail, Nucl. Austin, Tex. 1 (2010) 264–272, doi:http://dx.doi.org/10.4161/nucl.1.3.11799.
[50] H.L. Yin, T.P. Stossel, Control of cytoplasmic actin gel–sol transformation by gelsolin, a calcium-dependent regulatory protein, Nature 281 (1979) 583–586.
[51] I. Park, C. Han, S. Jin, B. Lee, H. Choi, J.T. Kwon, et al., Myosin regulatory light chains are required to maintain the stability of myosin II and cellular integrity, Biochem. J. 434 (2011) 171–180, doi:http://dx.doi.org/10.1042/bj20101473.
[52] E. Daimon, Y. Shibukawa, Y. Wada, Calponin 3 regulates stress fiber formation in dermal fibroblasts during wound healing, Arch. Dermatol. Res. 305 (2013) 571–584, doi:http://dx.doi.org/10.1007/s00403-013-1343-8.
[53] M. Ashburner, C.A. Ball, J.A. Blake, D. Botstein, H. Butler, J.M. Cherry, et al., Gene ontology: tool for the unification of biology. The gene ontology consortium, Nat. Genet. 25 (2000) 25–29, doi:http://dx.doi.org/10.1038/75556.
[54] S. Zhao, W. Xu, W. Jiang, W. Yu, Y. Lin, T. Zhang, et al., Regulation of cellular metabolism by protein lysine acetylation, Science 327 (2010) 1000–1004, doi: http://dx.doi.org/10.1126/science.1179689.
[55] S. Clavier, X. Du, S. Sagan, G. Bolbach, E. Sachon, An integrated cross-linking-MS approach to investigate cell penetrating peptides interacting partners, EuPA Open Prot. 3 (2014) 229–238, doi:http://dx.doi.org/10.1016/j.euprot.2014.03.002.
[56] M. Gstaiger, R. Aebersold, Applying mass spectrometry-based proteomics to genetics, genomics and network biology, Nat. Rev. Genet. 10 (2009) 617–627, doi:http://dx.doi.org/10.1038/nrg2633.